

Figure 1S. Photographs of metal depositions on glass slides

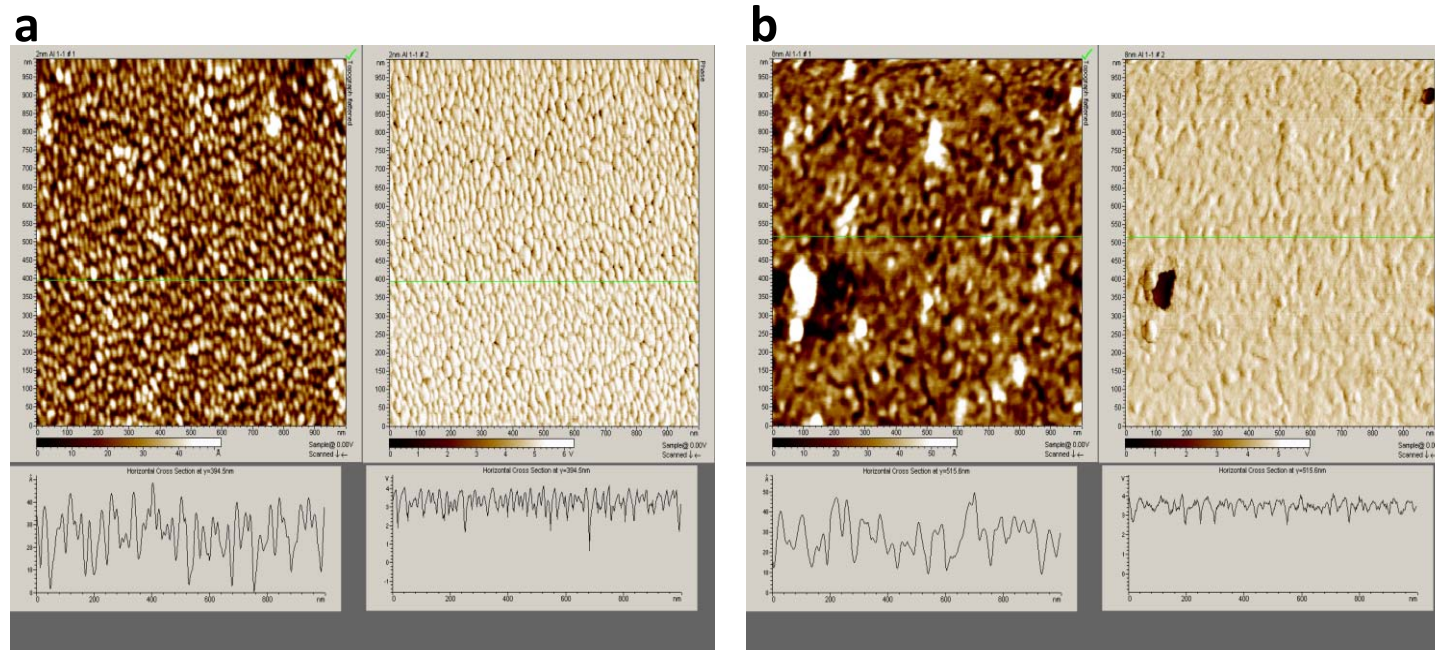


Figure 2S. (a) AFM images of 2 nm Al on glass (Left). Phase images (Right). Below are the respective line scans for the AFM images. (b) AFM images of 6 nm Al on glass (Left). Phase image (Right). Below are the respective line scans for the AFM images.

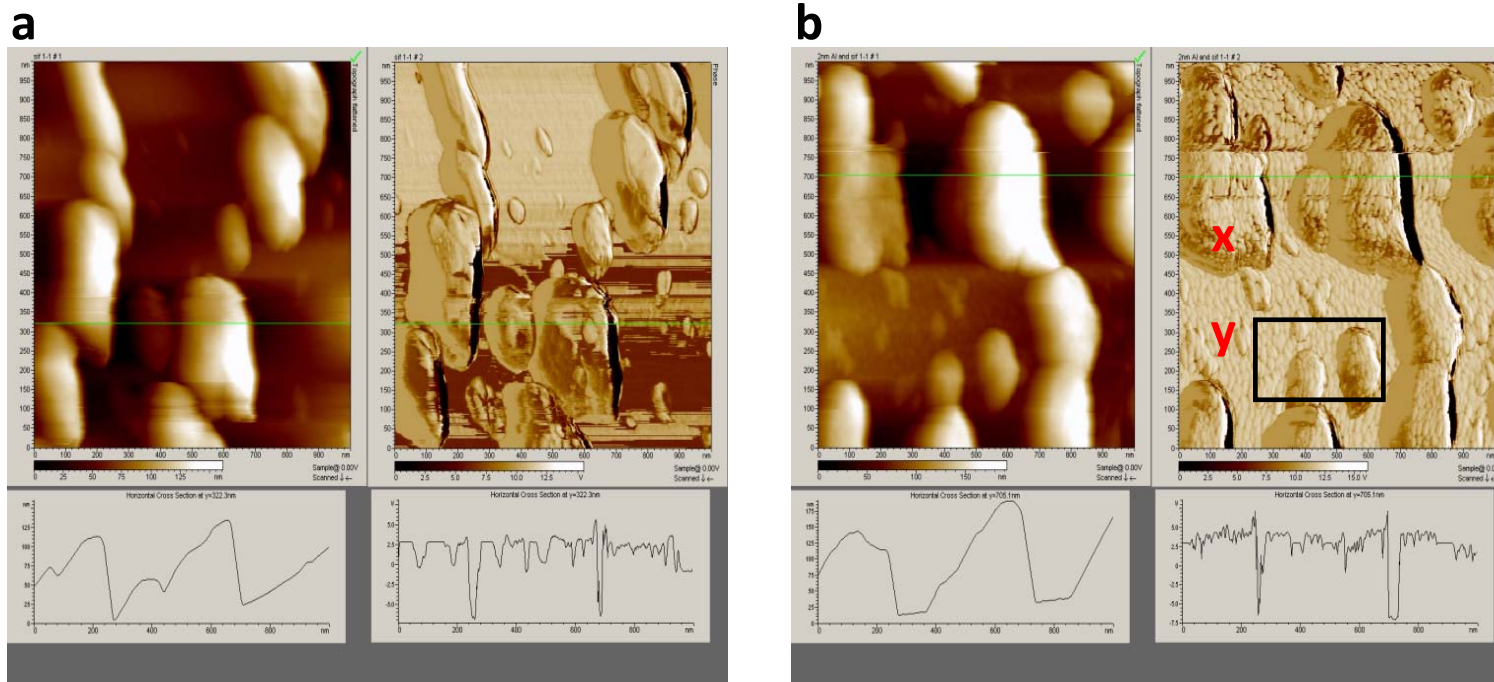


Figure 3S. (a) AFM images of SiFs (Left). Phase image (Right). Below are the respective line scans for the responding AFM images. (b) AFM images of 2 nm Al on SiFs (Left), phase image (Right). Below are the respective line scans for the AFM images.

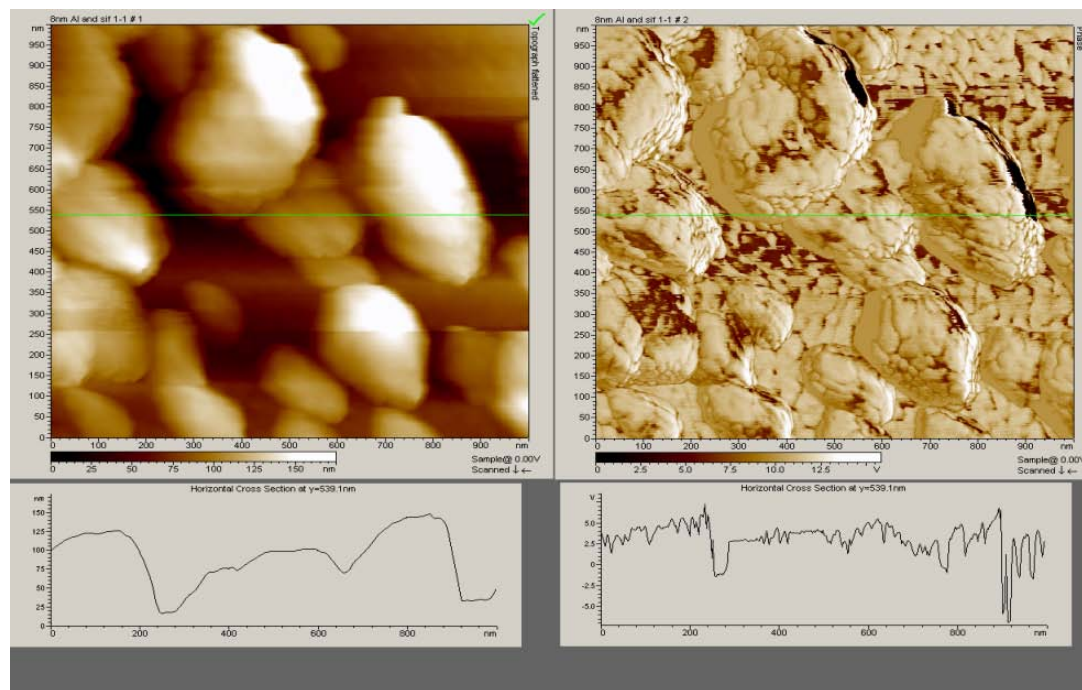


Figure 4S. AFM images of 8 nm Al on SiFs (Left). Phase image (Right). Below are the respective line scans for the AFM images.

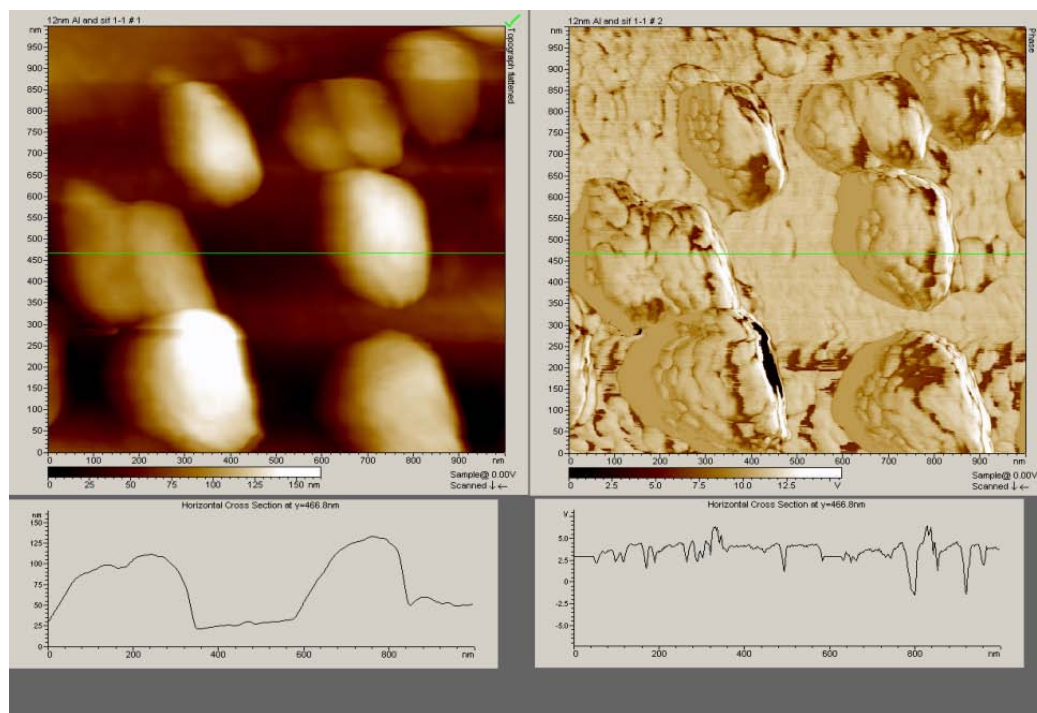


Figure 5S. AFM images of 12 nm Al on SiFs (Left). Phase image (Right) Below are the respective line scans for the AFM images.

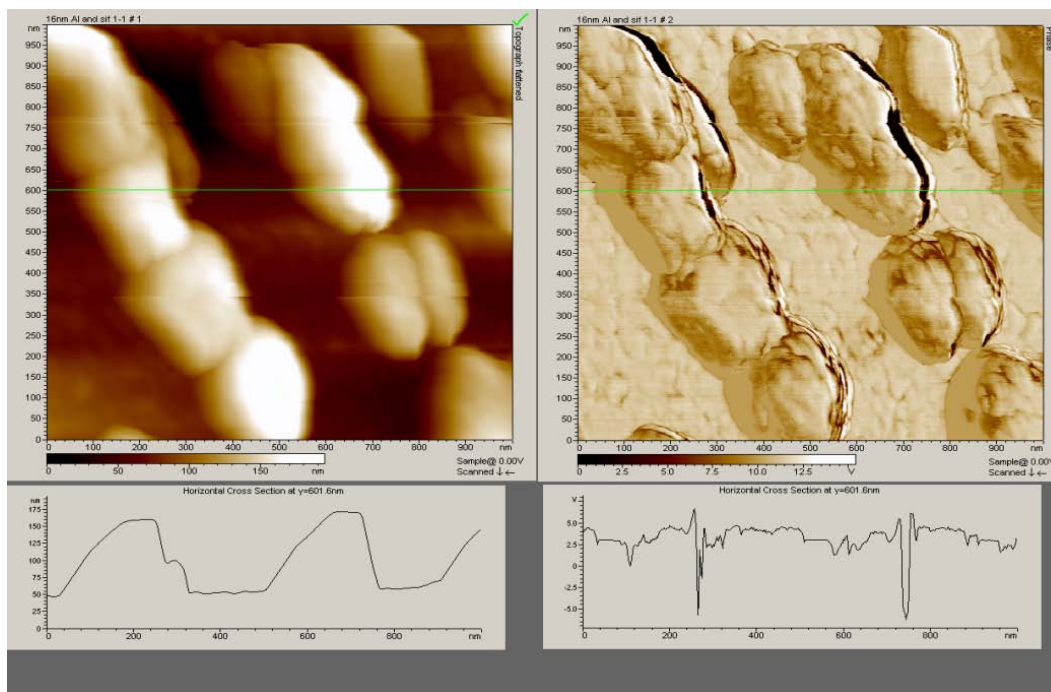


Figure 6S. AFM images of 16 nm Al on SiFs (Left). Phase image (Right). Below are the respective line scans for the AFM images.

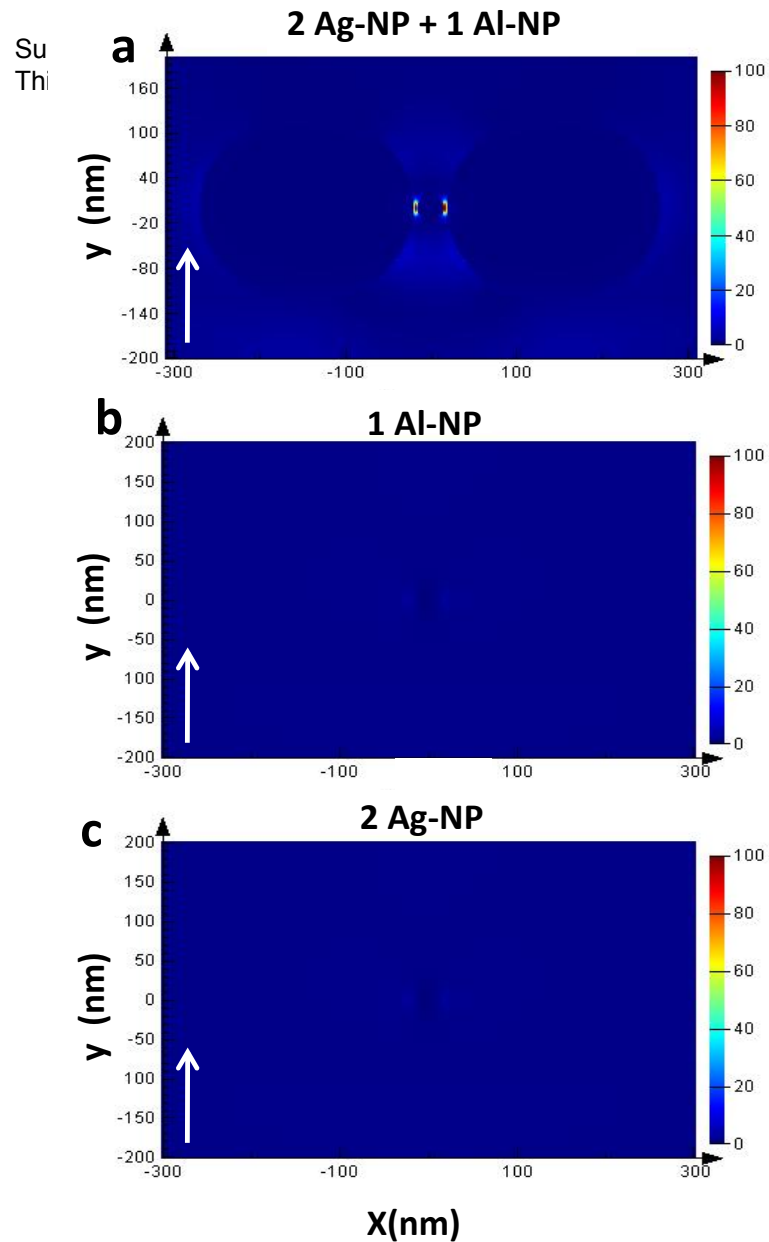


Figure 7S. E-field around Al- and Ag-NPs normalized to the same near-field $|\epsilon|^2$ intensity. Insertion of 30 nm Al NP between 250 nm Ag NPs enhances E-field 4-5-fold not only between NPs but also surrounding the particles.

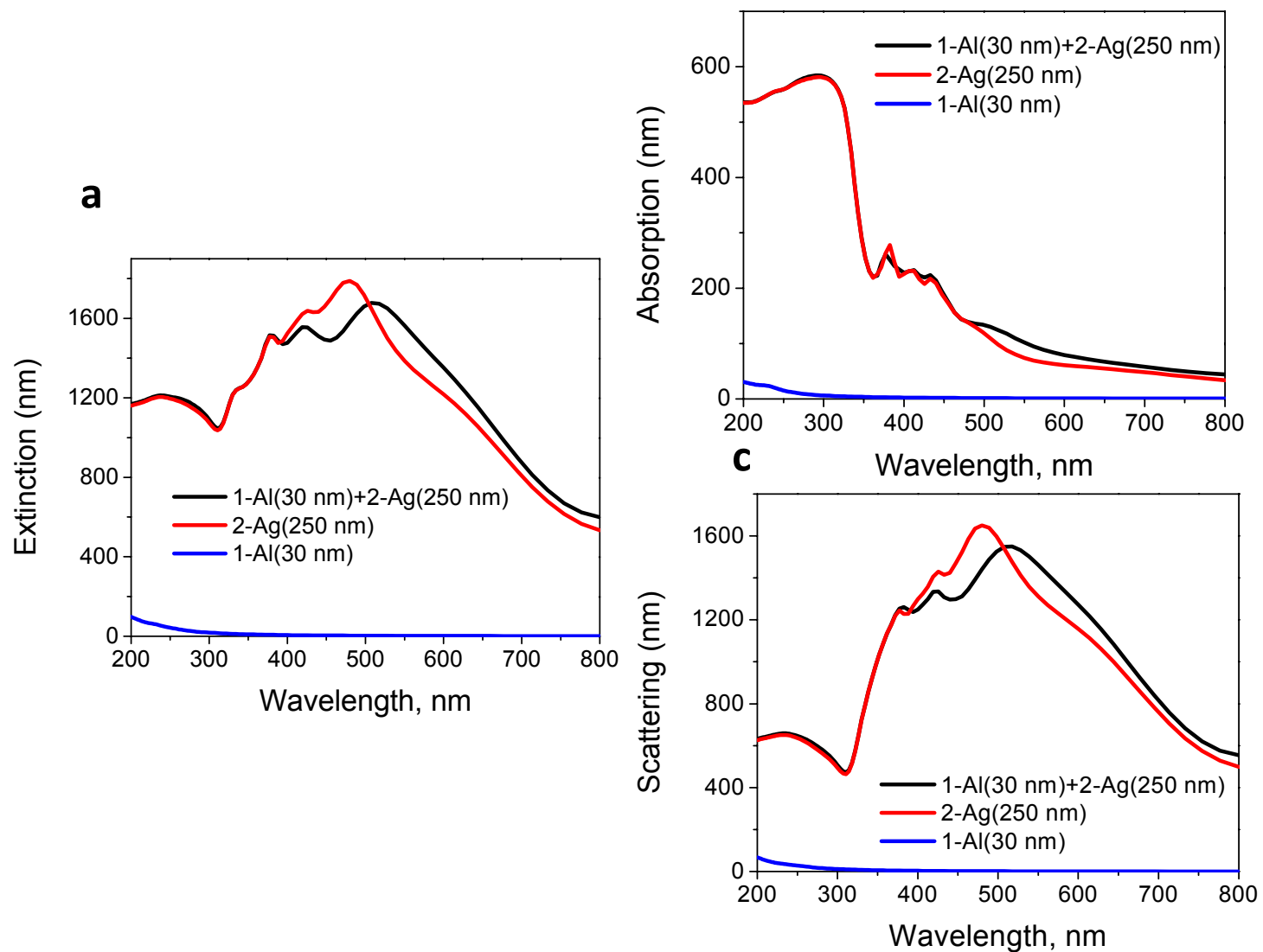


Figure 8S. (a) Extinction (absorption(b) + scattering(c)) spectra of NPs in water, based on Figure 5.

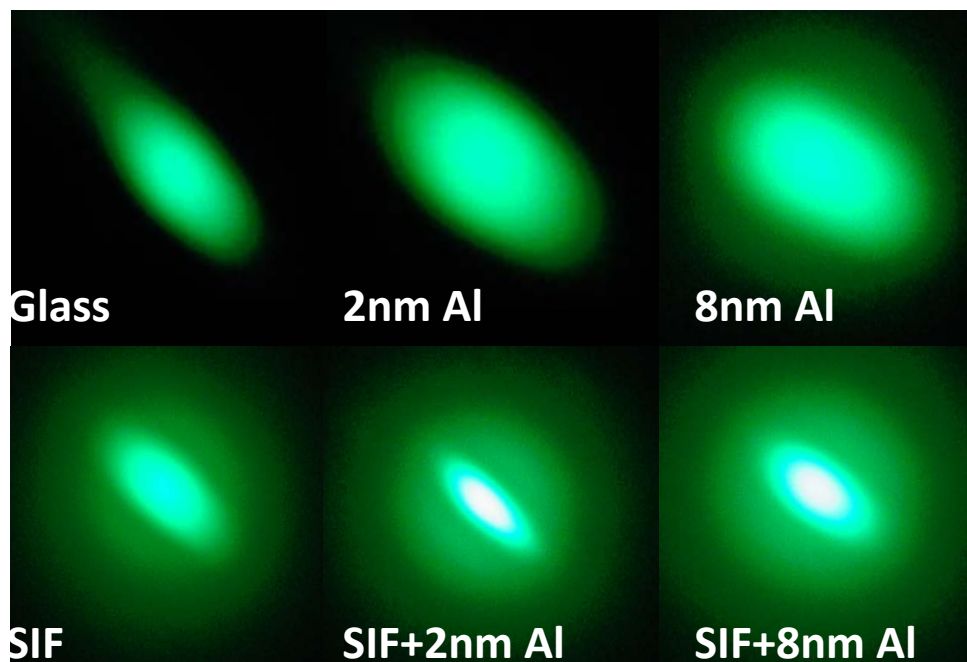


Figure 9S. Photographs of Fluorescein emission from the different metallic surfaces. Excitation was at 473 nm (laser line) and emission was collected through a long pass filter.

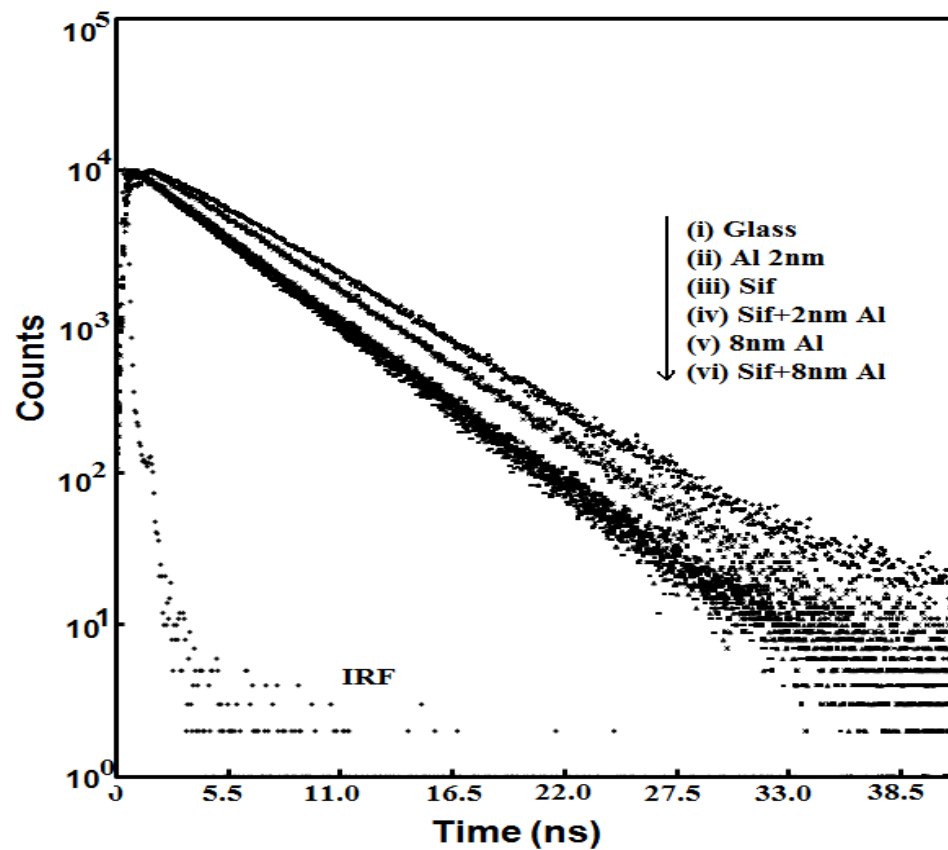


Figure 10S. Decay curves of Sodium Fluorescein in water [concentration $10^{-4}\mu\text{M}$] from the different metal depositions.

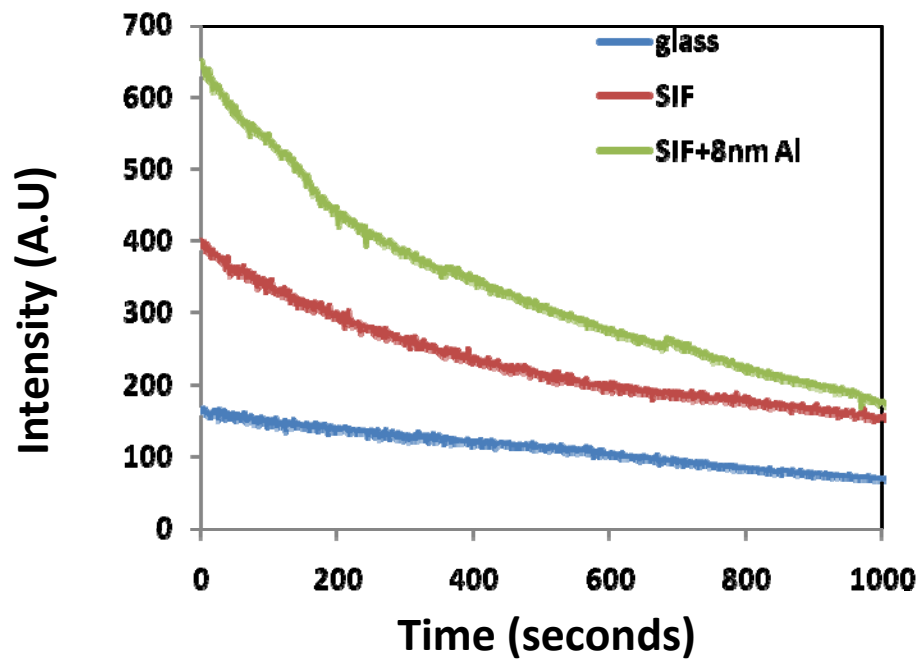


Figure 11S. Steady-state intensity decays (photostability) of fluorescein emission from metal slides and glass (control).